RESEARCH PAPER

Cyclodextrin-conjugated nanocarrier for magnetically guided delivery of hydrophobic drugs

Shashwat S. Banerjee · Dong-Hwang Chen

Abstract A magnetic nanosystem that simultaneously implements the cyclodextrin–drug complexation power, bioadhesive property of gum arabic (GA) and inherent magnetic properties of Fe_3O_4 nanoparticles, has recently been reported. In this study, a magnetic nanocarrier was fabricated by conjugating 2-hydroxypropyl-cyclodextrin (HCD) onto the gum arabic modified magnetic nanoparticles (GAMNP). The analyses of transmission electron microscopy (TEM) and dynamic light scattering (DLS) revealed that the product had a mean diameter of 14.8 nm and a mean hydrodynamic diameter of 29.3 nm. This nanocarrier showed good loading efficiency for ketoprofen. In addition, the in vitro release profile of ketoprofen from HCD-GAMNP was characterized by an initial fast release followed by a delayed release phase. In view of the better biocompatibility and the combined properties like specific targeting, complexation ability with hydrophobic drugs makes the nanosystem an exciting prospect for drug delivery.

Keywords Magnetic · Nanosystem · Hydroxypropyl-cyclodextrin · Hydrophobic drug · Delivery · Ketoprofen · Nanomedicine

S. S. Banerjee · D.-H. Chen (✉)
Department of Chemical Engineering, National Cheng Kung University, Tainan 701, Taiwan, ROC
e-mail: chendh@mail.ncku.edu.tw

Introduction

Nanochemistry offers exciting opportunities for design and fabrication of a wide variety of nanocarriers with multiple applications for nanomedicine, an emerging interdisciplinary field that utilizes nanostructures for diagnostics, targeted drug delivery, and real-time monitoring of therapeutic functions. Research into drug delivery and targeting systems based on nanomaterials is at the forefront of nanomedicine. An ambitious goal of drug delivery is to externally "remote control" the drug carriers in order to achieve the goal of maximum target specificity. One way to achieve this is by the introduction of magnetic properties in the drug carriers, followed by manipulating the pharmacodynamics of the carrier with an external magnetic field (Cinteza et al. 2006).

Iron oxide magnetic nanoparticles (MNPs) are an emerging form of nanomedicine for the treatment of various diseases since they can effectively perform as a magnetic field guided drug delivery vehicles (Lee et al. 2007; Kohler et al. 2005; Nasongkla et al. 2006; Jeong et al. 2007). MNPs as drug delivery vectors provide the ability to selectively target the desired organs or tissues inside the body, as well as accumulate a certain concentration of nanoparticles along the therapy path while the medication is released and acts locally by means of the application of an external magnetic field (Jurgons et al. 2006; Takada 2006). Therefore, the dosage of the medication can be reduced and the systemic side effect of the drugs kept

to a minimum. For biomedical applications, the biocompatibility of the MNPs, especially the shell, is essential. Therefore, it is necessary to engineer the surface of the nanoparticle to withstand harsh physiological conditions. Several synthetic and natural polymers have been employed to coat the surface of MNP (Lee et al. 2007).

Gum arabic (GA) is a natural polymer with mucoadhesive property which helps to fulfill some desirable features of a controlled drug delivery system like localization in specified regions to improve and enhance the bioavailability of the drug (Takada 2006). On the other hand, cyclodextrins form a whole new family of pharmaceutical excipients which have a doughnut-shaped structure with a hydrophilic outer surface and a lipophilic cavity, where poorly water-soluble molecules can shelter their most hydrophobic parts (Bender and Komiyama 1978; Saenger 1984).

Recently, we reported successful designing of a drug delivery vehicle with cumulative effects of the inclusion property of cyclodextrin, the bioadhesive property of GA as well as the magnetic property of iron oxide. The cyclodextrin employed in that study was β-cyclodextrin (CD) (Banerjee and Chen 2007a). We demonstrated from the loading and release experiments for drug-like ketoprofen that the system can be a promising vehicle for the administration of hydrophobic drugs. However, the cyclodextrin used in the system i.e., β-cyclodextrin faces several shortcoming in parenteral applications due to its low aqueous solubility and adverse effects like nephrotoxicity (Brewster and Loftsson 2007). In the current study, therefore, we explored the potential of using hydroxypropyl-β-cyclodextrin (HCD), one of the most important pharmaceutically relevant cyclodextrin derivatives for fabrication the drug delivery system. HCD have found growing interest in the field of novel pharmaceutical applications as it offers several advantages over natural cyclodextrins, like CD. HCD was much more water-soluble and more toxicologically benign than the CD in parenteral application (Gould and Scott 2005; Brewster et al. 2007). The size, structure, surface charge, and binding with HCD were characterized by transmission electron microscopy (TEM), dynamic light scattering (DLS), Fourier transform infrared (FTIR) spectroscopy, and thermogravimetric analysis (TGA). To demonstrate the applicability of the system as an efficient drug nanocarrier, we investigated the inclusion complexation

ability of HCD grafted magnetic nanocarrier with hydrophobic drugs-like ketoprofen in detail. Furthermore, we studied the influence of surfactant in the complexation ability of HCD grafted magnetic nanocarrier for ketoprofen. Finally, the ketoprofen in vitro release profile from these nanoparticles was studied.

Experimental

Materials

2-Hydroxypropyl-β-cyclodextrin (HCD) was purchased from Fluka (Buchs). Citric acid was obtained from Riedel-deHaën (Seelze). Ketoprofen and carbodiimide were procured from Sigma-Aldrich Chemical Co. (Germany). The water used throughout this work was the reagent-grade water produced by a Milli-Q SP ultra-pure-water purification system from Nihon Millipore Ltd., Tokyo. All other chemicals were of analytical grade and used without further purification.

Fabrication of GAMNP

Fe_3O_4 nanoparticles were prepared by co-precipitating Fe^{2+} and Fe^{3+} ions with ammonia solution and treating under hydrothermal conditions according to our previous work (Liao and Chen 2002). For the surface modification of Fe_3O_4 nanoparticles with GA, we have followed the procedure mentioned in our previous work (Banerjee and Chen 2007b). About 1.0 g of Fe_3O_4 nanoparticles were added into 100 mL of GA solution (5 mg/mL) in a stoppered bottle. The reaction mixture was sonicated for 20 min and then mixed on a vortex mixer for 5 min, and again sonicated for another 10 min. The resultant gum arabic modified magnetic nanoparticles (GAMNP) were recovered from the reaction mixture by placing the bottle on a permanent magnet with a surface magnetization of 6000 G. They settled within 1–2 min, then were washed three times with 100 mL of water, and finally dried in an air oven at 50 °C for 24 h and stored in a stoppered bottle for further use.

Synthesis of HCD-GAMNP

2-Hydroxypropyl-β-cyclodextrin (HCD) grafted GAMNP (HCD-GAMNP) was prepared by grafting 2-hydroxypropyl-β-cyclodextrin-citrate   (HCD-citrate)

Fig. 1 A scheme for the fabrication of HCD-GAMNP using HCD-citrate as a source

HCD - GAMNP
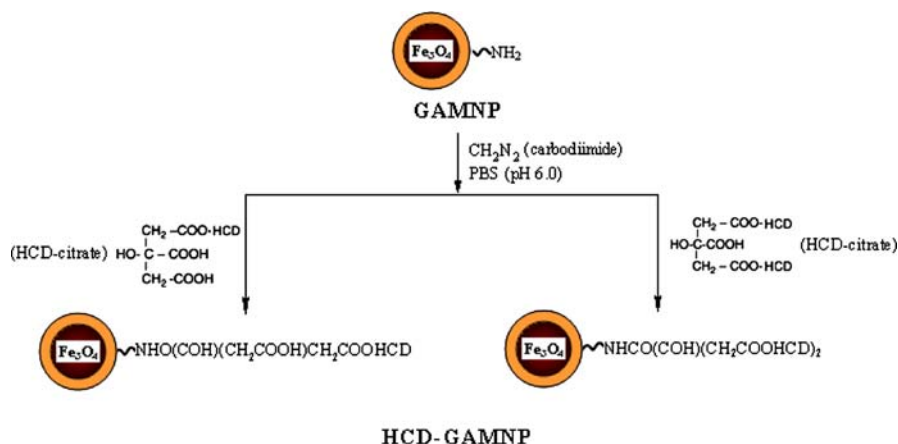
on GAMNP as illustrated in Fig. 1. HCD-citrate was synthesized by esterifying HCD with citric acid using the semidry reaction as reported in our previous work (Banerjee and Chen 2007a). About 3.0 g of HCD was mixed with 1.8 mL of water containing 1.02 g citric acid and the mixture was allowed to react in a circulating air oven at 105 °C for 3 h. The cured samples were purified by repeated washing with isopropanol in order to remove unreacted components as well as any soluble fragments or byproducts, followed by drying at 60 °C for 24 h. After drying, the HCD-citrate was stored in an air tight container for further use.

Conjugation of HCD-citrate with GAMNP was done by following the method described in our previous work (Banerjee and Chen 2007a). First, 1.0 g of Fe_3O_4 nanoparticles was added to 10 mL of buffer A (0.003 M phosphate, pH 6, 0.1 M NaCl) and sonicated for 10 min. About 5.0 mL of carbodiimide solution (0.025 g/mL in buffer A) was added and the reaction mixture was sonicated for another 10 min. Finally, 0.5 g of HCD-citrate was added to the above reaction mixture and sonicated for further 45 min. The HCD-citrate grafted GAMNP were recovered from the reaction mixture by placing the bottle on a permanent magnet with a surface magnetization of 6000 G. The magnetic particles settled within 1–2 min and then were washed repeatedly with deionized water followed by ethanol and finally with deionized water before vacuum drying.

Characterization

The size and morphology of the synthesized nano-carrier were investigated by TEM carried out on a Hitachi Model H-7500 at 120 kV. Colloidal suspensions were deposited directly onto a Formvar-covered copper grid and evaporated in air at room temperature. IR spectra were recorded on a Varian FTS-1000 FTIR spectrometer in a nitrogen purged environment. The hydrodynamic diameter was measured by DLS using a Malvern Autosizer 4700/PCS100 spectrometer equipped with an Ar ion laser operating at 488 nm. TGA was carried out on a Shimadzu TA-50WSI TGA with a heating rate of 10 °C/min.

Inclusion studies

Stock solutions of ketoprofen in water (1.25 mM) were prepared by first dissolving the drug in water of pH 11.0, and then pH of the solution was slowly reduced to 6.8 by adding a few drops of 0.1 M hydrochloric acid. The ketoprofen–HCD complex formation was investigated by taking precisely 25 mg of HCD-GAMNP in 5 mL of ketoprofen solutions of different concentration (0.0125–1.25 mM) at pH 6.8 and 398 K. The solutions were stirred on a horizontal laboratory shaker (200 rpm) for 24 h (which was the time required for equilibration to be reached) and then the MNPs were isolated from the solution by magnetic separation. The concentrations of ketoprofen in the solutions were determined using a spectrophotometer at 260 nm. Each experiment was repeated twice to ensure the reproducibility. The solution pH was adjusted by dilute NaOH or HCl.

Drug release study

The release rate experiments were performed in a glass apparatus at 310 K ± 0.5 K in phosphate buffer
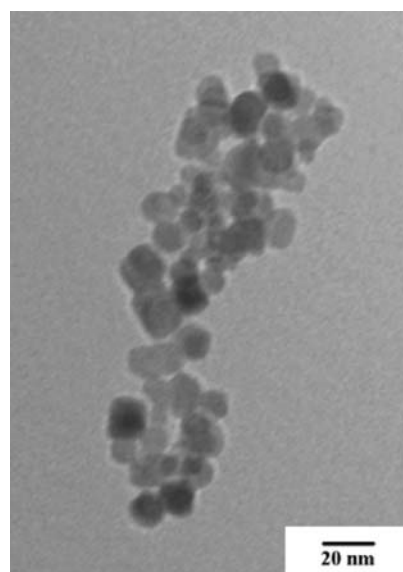
(7.4) solutions. HCD-GAMNP (250 mg) containing a known amount of ketoprofen were suspended in 50 mL of release medium and stirred in a laboratory stirrer and maintained at 310 ± 0.5 K in a water bath. Samples (1 mL) were periodically removed and assayed. The volume of each sample withdrawn was replaced by the same volume of fresh medium. The amount of released ketoprofen was analyzed with spectrophotometer at 260 nm. The drug release study was performed in duplicate.

Results and discussion

Characterization of HCD-GAMNP

The morphology and particle size distribution of HCD-GAMNP examined by TEM are shown in Fig. 2. The mean diameter of HCD-GAMNP estimated from the TEM image was found to be 14.8 nm. In our previous work (Banerjee and Chen 2007b), it was observed that MNPs which had a mean diameter of 13.2 nm on modification with GA led to the formation of secondary particles with a mean diameter of 34.2 nm. The results revealed that that the diameter of HCD-GAMNP was smaller than that of GAMNP while close to that for MNP which suggests that HCD grafting had resulted in the de-agglomeration of secondary particles. This might be due to the change in the surface functional groups of GAMNP

by the grafting of HCD as observed in the case of CD-GAMNP (Banerjee and Chen 2007a). DLS measurement revealed that HCD-GAMNP had a narrow hydrodynamic diameter distribution as indicated in Fig. 3. The resultant nanoparticles were mostly in the range of 17.7–56.1 nm with the rest accounting for less than 2.0%. The mean hydrodynamic diameter was estimated as 29.3 nm, which was larger than the mean diameter observed by TEM
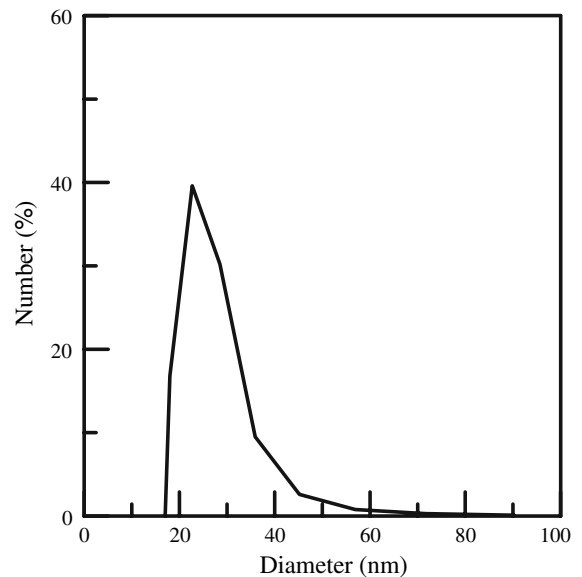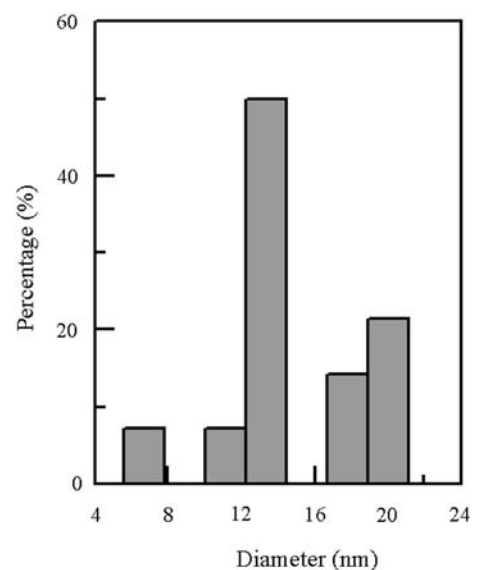
Fig. 3 Hydrodynamic diameter distribution of HCD-GAMNP

Fig. 2 Typical TEM image and particle size distribution of HCD-GAMNP

(14.8 nm). This revealed that HCD-GAMNP agglomerated in the aqueous media mainly due to the interaction between the outer hydroxyl group of HCD and the carboxylic group of GA. The mean hydrodynamic diameter of HCD-GAMNP was found to be smaller than GAMNP which had a mean hydrodynamic diameter of 36.8 nm as observed in our previous work (Banerjee and Chen 2007b). The smaller hydrodynamic diameter of HCD-GAMNP could be attributed to the different surface state of HCD-GAMNP as compared to GAMNP due to the presence of some unreacted carboxylic groups of citrate and the hydroxyl groups present on the outer surface of HCD (Banerjee and Chen 2007a).

The grafting of HCD on GAMNP was established by FTIR spectroscopy. The IR spectra of HCD, HCD-citrate, HCD-GAMNP, and GAMNP were analyzed using ATR-IR technique as shown in Fig. 4. Spectra of both HCD and HCD-citrate showed all the characteristic peaks of HCD at 941, 1028, and 1157 cm^{-1} and were quite alike. The peak at 941 cm^{-1} corresponds to R-1,4-bond skeleton vibration of CD. The peaks at
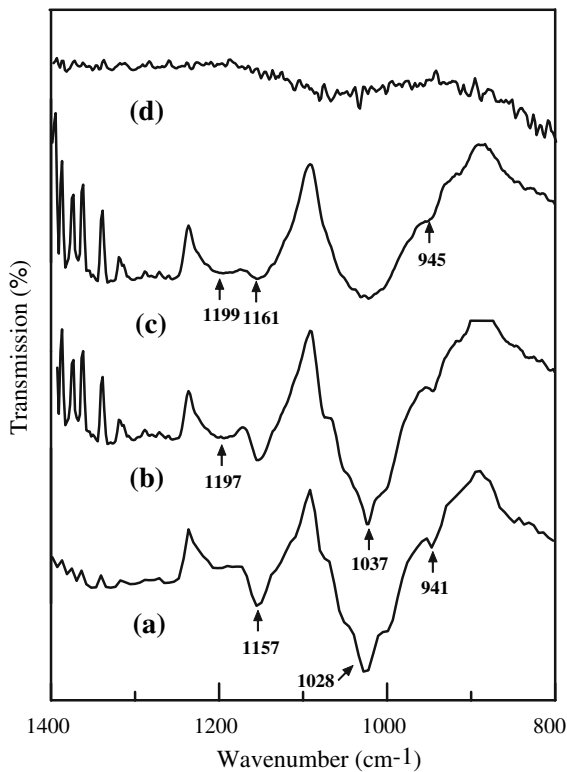
1,028 and 1,197 cm^{-1} related to the antisymmetric glycosidic v_a(C–O–C) vibration and the coupled v(C–C/C–O) stretch vibration. The prominent peak in the spectrum of HCD-citrate at 1,197 cm^{-1} could be referred to the HCD linkage to citrate. Furthermore, on comparison of the IR spectra, it was obvious that the spectrum of HCD-GAMNP showed a drastic change as compared to that of GAMNP. All the significant peaks of HCD in the range of 1,200–900 cm^{-1} were present in the spectrum of HCD-GAMNP with a small shift. On the basis of all these evidence, it could be concluded that HCD has been grafted on GAMNP (Loftsson and Masson 2001; Nelles et al. 1996).

Thermogravimetric analysis of GAMNP, HCD-GAMNP, and HCD-citrate were conducted to estimate the amount of HCD attached on the surface of GAMNP. As shown in Fig. 5, the TGA curve of GAMNP showed two stages of weight loss over the range of 30–900 °C. The first weight loss of about 2.22% in the temperature range of 30–150 °C might be due to the loss of residual water in the sample. The second weight loss of about 3.52% in the region of 150–340 °C was due to decomposition of GA. On the other hand, for HCD-GAMNP the TGA curves showed considerable weight loss in the region of 150–400 °C. The change of weight percentage in the TGA curves of HCD-GAMNP was about 6.95% which was due to HCD-citrate and GA. After deducting the weight loss due to GA, the value of which was obtained from the GAMNP analysis, the weight loss due to the grafted HCD-citrate was estimated to be 3.43%. The amount of HCD grafted on the GAMNP was calculated as 30.08 mg/g.

Fig. 4 ATR-IR spectra of HCD (**a**), HCD-citrate (**b**), HCD-GAMNP (**c**), and GAMNP (**d**)
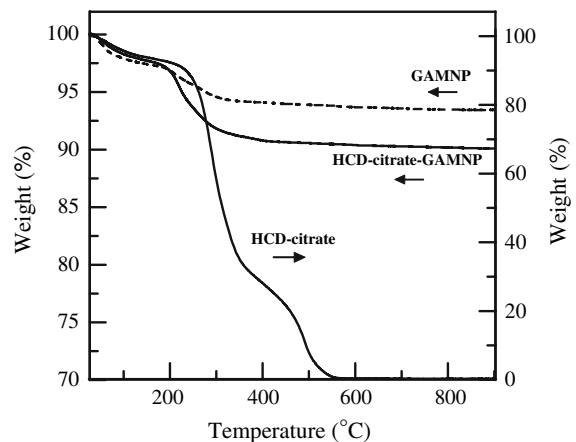

Fig. 5 TGA curves of GAMNP, HCD-citrate, and HCD-GAMNP

We have conducted the stability test of HCD-GAMNP by exposing it to the solutions of various pH (pH 2–10) with agitation on a horizontal laboratory shaker (200 rpm) for 24 h. By TGA, it was found that the amounts of HCD-citrate present on the surface before and after the treatment had no significant change, revealing the good stability of HCD-GAMNP.

Complexation of ketoprofen with GAMNP and HCD-GAMNP

The loading of ketoprofen by GAMNP and HCD-GAMNP was found to increase with increasing the initial concentration of ketoprofen in solution as shown in Fig. 6. The higher loading capability of ketoprofen by HCD-GAMNP was caused mainly due to the special hydrophobic cavity structure of HCD groups, which act as a host-guest complex with ketoprofen. The loading capacity of GAMNP for ketoprofen was found to be significantly low and the adsorption was caused possibly by n-d charge transfer between amino group of GA and ketoprofen molecule.

In order to gain more insight into the phenomenon of ketoprofen complexation by HCD-GAMNP, the adsorption equilibrium data were fitted with Langmuir isotherm equation which can be expressed as

$$\frac{C_e}{q_e} = \frac{C_e}{q_m} + \frac{1}{q_m K_L}, \tag{1}$$

where q_e is the equilibrium adsorption capacity of ketoprofen (mg/g), C_e is the equilibrium ketoprofen concentration in solution (mg/L), q_m is the maximum adsorption capacity (mg/g), and K_L is the Langmuir
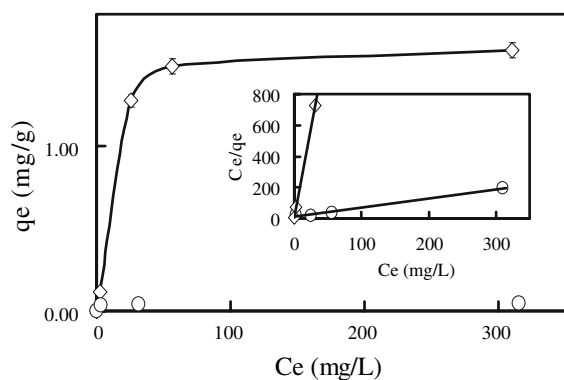

Fig. 6 Equilibrium isotherms for the adsorption of ketoprofen by GAMNP (○) and HCD-GAMNP (◇). The inset illustrates the corresponding linear dependences of C_e/q_e on C_e

adsorption equilibrium constant (L/mg). As indicated in the inset of Fig. 6, the plot of C_e/q_e versus C_e yielded a straight line, revealing that the adsorption of ketoprofen on HCD-GAMNP followed the Langmuir adsorption isotherm. From the slope and intercept, the values of q_m and K_L could be determined as 1.68 mg/g and 0.06 L/mg for HCD-GAMNP and 0.043 mg/g and 12.74 L/mg for GAMNP, respectively. The maximum loading of ketoprofen observed in case of CD-GAMNP was found to be 2.72 mg/g (Banerjee and Chen 2007a). The higher loading capacity of ketoprofen with CD-GAMNP as compared to HCD-GAMNP can be explained on the basis of the solvation sphere bound strongly to the carboxyl group of ketoprofen which reduces the interaction affinity between ketoprofen and CD. This phenomenon was more intense in the case of HCD due to the presence of extended solvation sphere of hydroxypropyl group which may result in a reduced amount of complexation between HCD and ketoprofen (Rozou et al. 2005).

Effect of temperature

The effects of temperature on inclusion of ketoprofen by HCD-GAMNP were investigated at a temperature range of 278–318 K and at an initial ketoprofen concentration of 0.25 mM. As shown in Fig. 7a, the loading capacity of ketoprofen by HCD-GAMNP decreased with increase in temperature, revealing the exothermic nature of the inclusion processes. The corresponding enthalpy and entropy changes (ΔH and ΔS) of the studied complexes were determined from the van't Hoff plots (Junquera and Aicart 1997), $\ln(q_e/C_e)$ versus $1/T$ as shown in Fig. 7b. The ΔH value calculated from the slope was found to be −46.41 kJ/mol, and ΔS calculated from the intercept was found to be −184.63 J/molK. It can be observed from the results that in the complex formation of ketoprofen with HCD-GAMNP, ketoprofen binds with a favorable enthalpic term ($\Delta H < 0$) and an unfavorable entropic term ($\Delta S < 0$).

Effect of the presence of surfactant

For solubilization of drugs, the most common techniques employed by a formulation scientist to enhance the solubility of a hydrophobic drug involve in situ salt formation (pH-adjustment), or by use of
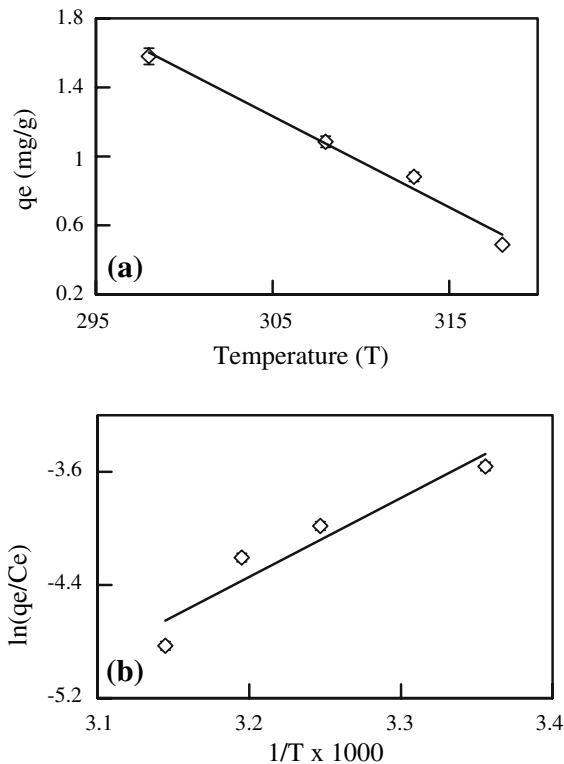
Fig. 7 Effects of temperature on ketoprofen inclusion by HCD-GAMNP (a) and the plots of $\ln(q_e/C_e)$ against $1/T$ for HCD-GAMNP (b)

additives such as complexing agents, surfactants, and co-solvents. However, very few studies on the combine impacts of surfactants and HCD-conjugated nanoparticle on drug loading have been reported (Rao and Nerurkar 2006). Therefore, the effect of the presence of surfactant on the inclusion of ketoprofen by HCD-GAMNP was studied by taking a solution of surfactant (sodium dodecyl sulfate—SDS) and ketoprofen, and varying the concentration of SDS (0.05–0.20 mM) while keeping the concentration of ketoprofen constant (0.25 mM). The concentration of SDS was kept below the critical micelle concentration to avoid the possibility of solubilization of ketoprofen in the solution by formation of miscelles.

It was observed that the inclusion of ketoprofen by HCD-GAMNP was 1.58 mg/g in the absence of SDS, but decreased to 1.11, 0.70, and 0.14 mg/g when 0.05, 0.10, and 0.20 M of SDS were present, respectively. The decrease in inclusion of ketoprofen with increasing concentration of SDS could be due to the different shapes of SDS and ketoprofen. Catena

and Bright (1989) reported that CD molecule preferred to approach the substrate equatorially as opposed to axially, and hence the more linear compound found the entry in the hydrophobic cavity by equatorial approach more favorable than less linear compound which was hindered during the inclusion process. SDS molecules are more linear as compared to ketoprofen, so they can enter the cavity of HCD more easily, and hence the majority of the cavity of HCD may be occupied by SDS molecules whose hydrophobic chain tends to reside by coiling in the hydrophobic cavity of HCD.

Controlled release

Figure 8 shows the release profile of ketoprofen loaded HCD-GAMNP (1.58 M of ketoprofen per g of HCD-GAMNP) as a function of time. The profile showed an initial rapid release in the first 30 min and a slow and steady release in the followed period until equilibrium was reached after about 5 h. Complete release of drug is not observed may be due to the diffusion equilibrium that exists between the drug–HCD complex of HCD-GAMNP and the released drug in the solution which retards the complete drug release. From this result, we could speculate that, following administration, some of the encapsulated drug molecules will be rapidly released from HCD-GAMNP, whereas some will remain associated to HCD-GAMNP. At this level, the degradation of the particles, probably driven by the enzyme lysozyme (Sashiwa et al. 1990), could facilitate the delivery of the associated drug at the absorption site.
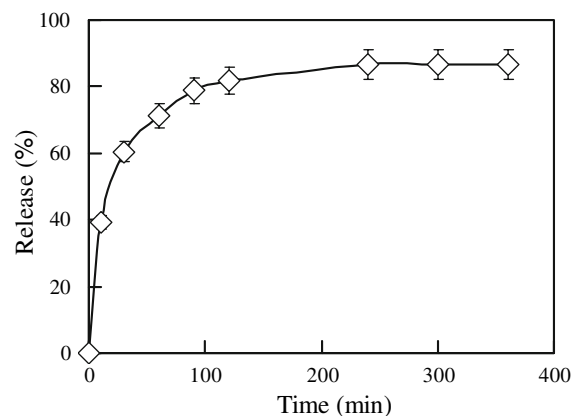

Fig. 8 Release profile of ketoprofen from HCD-GAMNP

Conclusions

We fabricated a magnetic nanocarrier by conjugation HCD with GA bound Fe_3O_4 nanoparticles to get a superior drug delivery nanovehicle with respect to biocompatibility. The nanosystem demonstrated the utility of HCD grafting on GAMNP for efficient loading of hydrophobic drug molecules like ketoprofen. The loading capacity of HCD-GAMNP for ketoprofen was found to be less that the loading capacity offered by β-cyclodextrin. The complexation of HCD-GAMNP with ketoprofen was found to be exothermic and enthalpy driven processes. The presence of surfactant (sodium dodecyl sulfate) in the ketoprofen solution showed that the inclusion of ketoprofen in HCD-GAMNP decreased. It can be because sodium dodecyl sulfate due to its linear structure find it easier to enter the HCD cavity equatorially as compared to less linear ketoprofen molecule, and hence the majority of the cavity of HCD gets saturated with sodium dodecyl sulfate molecule. The in vitro release profile of ketoprofen from HCD-GAMNP showed an initial fast release followed by a slow sustained release phase. Further modification of the synthesized nanocarrier to increase the drug loading ability is a possibility, which we are planning to develop an extension of this work. Thus, this nanocarrier may serve as a promising prototype for the administration of hydrophobic drugs.

References

Banerjee SS, Chen DH (2007a) Magnetic nanoparticles grafted with cyclodextrin for hydrophobic drug delivery. Chem Mater 19:6345–6349. doi:10.1021/cm702278u

Banerjee SS, Chen DH (2007b) Fast removal of copper ions by gum arabic modified magnetic nano-adsorbent. J Hazard Mater 147:792–799. doi:10.1016/j.jhazmat.2007.01.079

Bender M, Komiyama M (1978) Cyclodextrin chemistry. Springer, Berlin

Brewster ME, Loftsson T (2007) Cyclodextrins as pharmaceutical solubilizers. Adv Drug Deliv Rev 59:645–666. doi:10.1016/j.addr.2007.05.012

Brewster ME, Mackie C et al (2007) The use of solubilizing excipients and approaches to generate toxicology vehicles for contemporary drug pipelines. In: Augustijns P, Brewster ME (eds) Solvent systems and their selection in pharmaceutics and biopharmaceutics. American Association of Pharmaceutical Scientists and Springer, New York, pp 221–266

Catena GC, Bright FV (1989) Thermodynamic study on the effects of beta-cyclodextrin inclusion with anilinonaphthalenesulfonates. Anal Chem 61:905–909. doi:10.1021/ac00183a024

Cinteza LO, Ohulchanskyy TY et al (2006) Diacyllipid micelle-based nanocarrier for magnetically guided delivery of drugs in photodynamic therapy. Mol Pharm 3:415–423. doi:10.1021/mp060015p

Gould S, Scott RC (2005) 2-Hydroxypropyl-β-cyclodextrin (HP-β-CD): a toxicology review. Food Chem Toxicol 43:1451–1459. doi:10.1016/j.fct.2005.03.007

Jeong U, Teng X et al (2007) Superparamagnetic colloids: controlled synthesis and niche applications. Adv Mater 19:33–60. doi:10.1002/adma.200600674

Junquera E, Aicart E (1997) Potentiometric study of the encapsulation of ketoprophen by hydroxypropyl-β-cyclodextrin. Temperature, solvent, and salt effects. J Phys Chem B 101:7163–7171. doi:10.1021/jp963977s

Jurgons R, Seliger C et al (2006) Drug loaded magnetic nanoparticles for cancer therapy. J Phys Condens Matter 18:S2893–S2902. doi:10.1088/0953-8984/18/38/S24

Kohler H, Sun C et al (2005) Methotrexate-modified superparamagnetic nanoparticles and their intracellular uptake into human cancer cells. Langmuir 21:8858–8864. doi:10.1021/la0503451

Lee H, Yu MK, Park S, Moon S et al (2007) Thermally cross-linked superparamagnetic iron oxide nanoparticles: synthesis and application as a dual imaging probe for cancer in vivo. J Am Chem Soc 129:12739–12745. doi:10.1021/ja072210i

Liao MH, Chen DH (2002) Preparation and characterization of a novel magnetic nano-adsorbent. J Mater Chem 12:3654–3659. doi:10.1039/b207158d

Loftsson T, Masson M (2001) Cyclodextrins in topical drug formulations: theory and practice. Int J Pharm 225:15–30. doi:10.1016/S0378-5173(01)00761-X

Nasongkla N, Bey E et al (2006) Multifunctional polymeric micelles as cancer-targeted, MRI-ultrasensitive drug delivery systems. Nano Lett 6:2427–2430. doi:10.1021/nl061412u

Nelles G, Weisser M et al (1996) J Am Chem Soc 118:5039–5046. doi:10.1021/ja9539812

Rao VM, Nerurkar M (2006) Co-solubilization of poorly soluble drugs by micellization and complexation. Int J Pharm 319:98–106. doi:10.1016/j.ijpharm.2006.03.042

Rozou S, Michaleas S et al (2005) Study of structural features and thermodynamic parameters, determining the chromatographic behaviour of drug–cyclodextrin complexes. J Chromatogr A 1087:86–94. doi:10.1016/j.chroma.2005.02.039

Saenger W (1984) Inclusion compounds. Academic Press, London

Sashiwa H, Saimoto H et al (1990) Lysozyme susceptibility of partially deacetylated chitin. Int J Biol Macromol 12:295–296. doi:10.1016/0141-8130(90)90016-4

Takada K (2006) Oral formulation for gastrointestinal drug delivery. US Patent 7097851 B1